

Suppression of microRNA-9-5p rescues learning and memory in chronic cerebral hypoperfusion rats model

Na Wei^{1,2,3,*}, Kai Zheng^{4,*}, Rui Xue⁵, Sheng-Li Ma⁶, Hua-Yan Ren^{1,2,3}, Hui-Fen Huang^{1,2,3}, Wei-Wei Wang^{1,2,3}, Jing-Jing Xu^{1,2,3} and Kui-Sheng Chen^{1,2,3}

¹Department of Pathology, The First Affiliated Hospital of Zhengzhou University, Zhengzhou 450002, People's Republic of China

²Henan Key Laboratory of Tumor Pathology, Zhengzhou 450002, People's Republic of China

³Department of Pathology, School of Basic Medicine, Zhengzhou University, Zhengzhou 450002, People's Republic of China

⁴Department of Geriatrics, Tongji Hospital, Tongji Medical College, Huazhong University of Science and Technology, Wuhan 430030, China

⁵Medical Research Center, The First Affiliated Hospital of Zhengzhou University, Zhengzhou 450002, People's Republic of China

⁶Department of Emergency, The First Affiliated Hospital of Zhengzhou University, Zhengzhou 450002, People's Republic of China

*These authors have contributed equally to this work

Correspondence to: Jing-Jing Xu, **email:** xujingjing_1982@163.com
Kui-Sheng Chen, **email:** kuishengchen@zzu.edu.cn

Keywords: miR-9-5p; memory; chronic cerebral hypoperfusion; long-term potentiation

Received: May 12, 2017

Accepted: August 17, 2017

Published: November 11, 2017

Copyright: Wei et al. This is an open-access article distributed under the terms of the Creative Commons Attribution License 3.0 (CC BY 3.0), which permits unrestricted use, distribution, and reproduction in any medium, provided the original author and source are credited.

ABSTRACT

Chronic cerebral hypoperfusion has been associated with cognitive impairment in dementias, such as Alzheimer's disease (AD) and vascular disease (VaD), the two most common neurodegenerative diseases in aged people. However, the effective therapeutic approaches for both AD and VaD are still missing. MicroRNAs (miRNAs) are small non-coding RNAs that play important roles in the epigenetic regulation in many neurological disorders; the critical roles of miRNAderegulation had been implicated in both AD and VaD. In the current study, we reported that miR-9-5p is elevated in the serum and cerebrospinalfluid of patientswith VaD. The miR-9-5p wasalso increased in both the hippocampus and cortex of rats with 2-vessel occlusionsurgery. Furthermore, application ofmiR-9-5p antagomirs attenuated the memory impairments in rats with 2-vessel occlusion surgery both in the Morris water maze and inhibitory avoidance step-down tasks. Furthermore, miR-9-5p antagomirs reducedthe inhibition oflong-term potentiation and loss of dendritic spines in chronic cerebral hypoperfusionrats. Additionally, the cholinergic neuronal function was rescued by miR-9-5p antagomirs, as well as the neuronal loss and the oxidative stress. We concluded that miR-9-5p inhibition may be a potential therapeutic target for the memory impairments caused by chronic cerebral hypoperfusion.

INTRODUCTION

Dementia is a broad category of brain diseases that cause a long term and gradualdecrement in emotionsand memory, which is great enough to reduce a person's

ability to perform everyday activities [1]. There are severaltypes of dementia, including Alzheimer's disease (AD), vascular dementia (VaD), Lewy dody dementia (LBD), andfrontotemporal dementia (FTD) among others. Among them, AD and VaD are the two most prevalent

types, which account for more than 80% of the dementia cases [2].

In the brain of AD and VaD, the blood flow was reported to be reduced at an early stage and to be directly correlated with cognitive measures [3]. It is known that the flow of blood delivers the essential oxygen and nutrients to the brain cells and plays an important role in the maintenance of normal thinking, learning, and memory [4]. The dramatic blood flow reduction in patients with AD or VaD may potentially lead to brain cell damage and cognitive decline [5, 6]. Indeed, as a result of vascular risk factors such as hypertension, diabetes mellitus, hypercholesterolemia, and smoking, chronic cerebral hypoperfusion (CCH) is a common vascular component among AD risk factors [7]. In VaD, the deep brain areas, particularly white matter areas, suffer from chronic and moderate ischemia, which is a state representing one of the physiopathological mechanisms of damage [8]. Consistent with this, the microvessels in the AD and VaD brains are frequently narrowed, degenerated, and amyloid-laden, suggesting a pivotal role of cerebrovascular factors in both AD and VaD [9, 10]. Additionally, numerous studies have suggested that CCH might promote neurodegeneration through neuronal energy failure, production of reactive oxygen species, and proinflammatory cytokines by activated microglial cells that, in turn, damage the neuronal cells and contribute to white matter lesions [11].

MicroRNAs (miRNAs) are small (~22 nucleotides), endogenous noncoding RNA molecules that play important roles in diverse biological processes [12]. The mature miRNA is incorporated into the miRNA-induced silencing complex (miRISC) and then guides it to target sequences by recognizing their target sites located in 3'UTRs *via*

incomplete base-pairing. The binding of miRNA with its targets always leads to mRNA destabilization or translational repression of the target genes [13, 14]. The aberrant regulation of miRNA had been reported in both AD and VaD brains [15, 16]. Among them, miR-9, which is a highly conserved miRNA located on chromosome 3 in the mouse genome, is of particular interest. Previous studies suggested that miR-9 is enriched in the brain, especially during development [17]. In AD brains, the level of miR-9 is increased in the temporal lobes, neocortex, and hippocampal regions when compared with age-matched healthy adults [18, 19]. However, the role of miR-9 in the progression of memory impairment induced by vascular factors has not been studied yet.

In this study, we reported that miR-9-5p is upregulated in both the serum and cerebrospinal fluid of patients with VaD and in the hippocampus of CCH rats. Furthermore, reduction of miR-9-5p by antagomirs rescued the learning and memory ability, synaptic plasticity, dendritic spines, cholinergic neurons, oxidative stress level, and neuronal loss induced by CCH.

RESULTS

miR-9-5p is upregulated in patients with VaD and CCH rats

We first analyzed the miR-9-5p level in the serum and cerebrospinal fluid (CSF) of patients with VaD as described above. We found that in the serum of patients with VaD, the level of miR-9-5p increased to about 2.4 folds of age-matched controls (Figure 1A). A more prominent increment was found in the CSF samples (Figure 1B). As a miRNA control, the level of miR-16

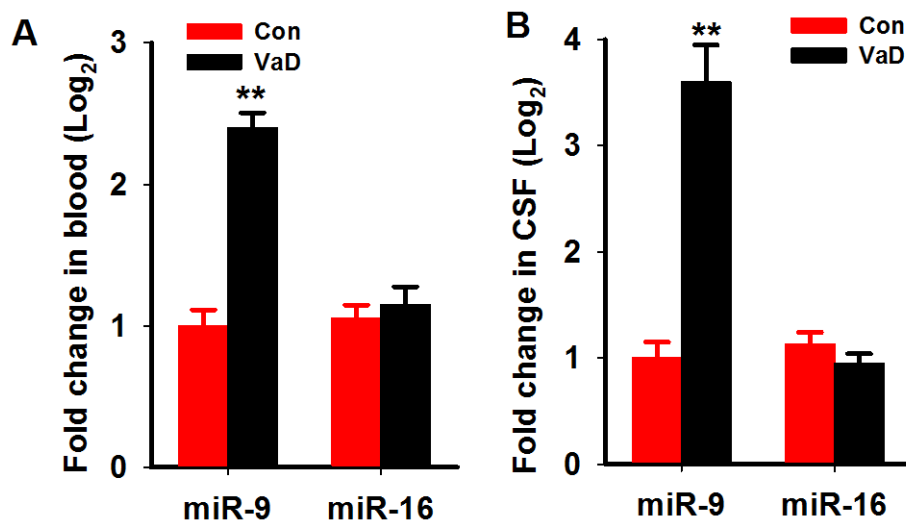


Figure 1: MiR-9-5p is upregulated in the serum and CSF of patients with VaD. The serum and CSF of patients with VaD and age-matched controls were collected as described in Methods. The level of miR-9-5p and miR-16 in the serum (A) and CSF (B) were detected by Q-PCR. CSF, cerebrospinal fluid; VaD, vascular dementia; **, $P < 0.01$, compared with the controls.

was not changed in both the serum and CSF (Figure 1A, 1B). We further examined the miR-9-5p level in the hippocampi and cortices of rats at 3 months after the 2VO surgery. As expected, we detected an increase in miR-9-5p levels both in the hippocampus and cortex of the CCH rats (Figure 2A, 2B). Similarly to our findings in patients, the levels of miR-16 were not changed but the levels of miR-181c were reduced in the CCH rats (Figure 2A, 2B). These data strongly suggested that miR-9-5p is upregulated in patients with VaD and CCH rats.

Reduction of miR-9-5p *in vivo* rescues learning and memory impairments in CCH rats

To understand the effects of miR-9-5p increment in the pathogenesis of VaD, we artificially suppressed the expression of miR-9-5p in the brains of the CCH rats with rno-miR-9-5p antagomir at 3 months after the surgery (Figure 3A). Subsequently, 2 weeks later, the spatial learning and memory abilities of the rats were evaluated with the MWM task. The swimming tracks of the rats revealed that the sham rats reached the platform in less than 20 s by using a direct searching strategy, while the CCH rats took over 40 s using a random searching strategy. Treating the rats with anti-miR-9-5p improved the searching strategy (Figure 3B). On the first 2 training days, we did not detect any significant difference among the groups. Beginning on training day 3, the escape latency of the CCH group was longer than that of the sham group, and treatment with anti-miR-9-5p significantly decreased the latency in the CCH+Anta-miR-9-5p group compared with the CCH group (Figure 3C). In the probe

trial, rats in the CCH group displayed less crossing times to the platform region and less duration and distance in the target quadrant than the sham group, while treatment with Anta-miR-9-5p improved these measures in CCH rats (Figure 3D-3F). No obvious difference was detected between the Con and Anta-miR-9-5p rats (Figure 3D-3F).

We used the step-down inhibitory avoidance test to evaluate the emotional cognition of the rats. During training, no significant differences were found in the step-down latency among the groups. In the test period, CCH rats showed obviously a shorter latency than control rats, while anti-miR-9-5p extended the latency of CCH rats (Figure 4A). We also calculated the errors in both the training and test periods and found that CCH rats made more errors in both stages, while anti-miR-9-5p reduced the number of errors (Figure 4B). No significant differences were found between the Con and Anta-miR-9-5p groups. The above results indicated that suppression of miR-9-5p is able to reverse the memory deficits in CCH rats.

Reduction of miR-9-5p *in vivo* rescues the synaptic impairments in CCH rats

Previous studies suggested that synaptic plasticity is the basis for learning and memory. We examined synaptic plasticity by evaluating LTP modifications in the hippocampus of CCH rats. We found that the CCH rats displayed decreased slope of EPSP, which were lower than the rats of the Sham group. Treatment with anti-miR-9-5p elevated the declined LTP induced by CCH

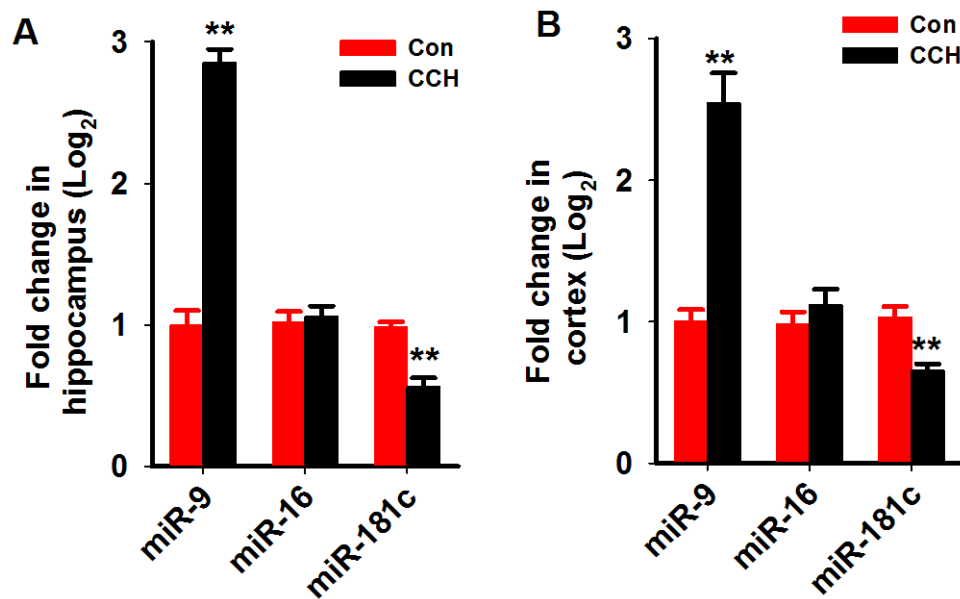


Figure 2: MiR-9-5p is increased in the hippocampus and cortex of CCH rats. Three months after the 2VO surgery, the hippocampus (A) and cortex (B) were extracted and the RNA was isolated. The levels of miR-9-5p and miR-16 were evaluated by Q-PCR by using specific primers. 2VO, 2-vessel occlusion; CCH, chronic cerebral hypoperfusion; **, $P < 0.01$, compared with Con rats.

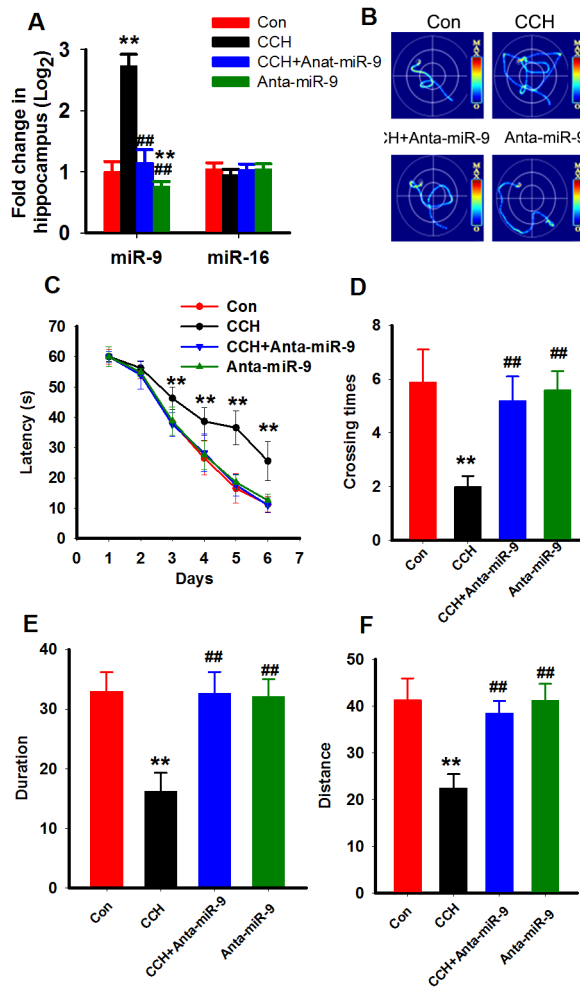


Figure 3: Inhibition of miR-9-5p rescued the spatial learning memory impairments of CCH rats. Three months after the surgery, Morris water maze was applied to evaluate the spatial memory of rats. (A) The miR-9-5p and miR-16 levels in different treated rats. ** $P < 0.01$, compared to control rats. ### $P < 0.01$, compared with CCH rats. (B) The representative escape traces for different groups in the final training day. (C) The latency during the six-days training task in the Morris water maze. (D-F) The total crossing times (D), the total time spent in the target quadrant (E), and the total swimming distances during the probe trial (F). CCH, chronic cerebral hypoperfusion; ** $P < 0.01$, compared with sham rats; ### $P < 0.01$, compared with CCH rats.

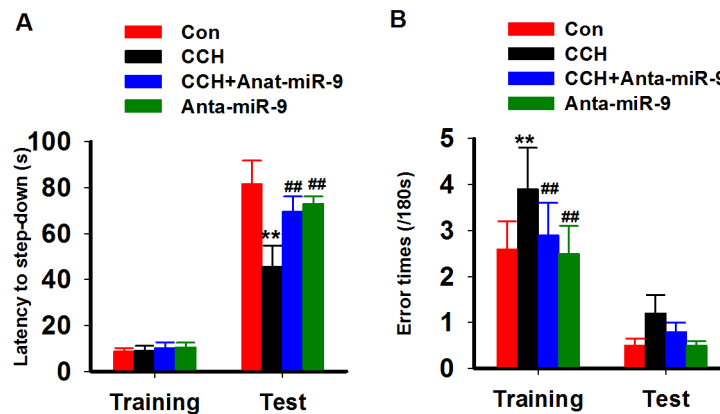


Figure 4: Inhibition of miR-9-5p rescued the fear memory impairments of CCH rats. The inhibitory avoidance tasks are applied to analyze fear memory of rats. After training, long-term memory test are carried at 24 h later. The step-down latency (A) and error times (B) were recorded. CCH, chronic cerebral hypoperfusion; ** $P < 0.01$, compared with Con rats; ## $P < 0.01$, compared with CCH rats.

(Figure 5A, 5B). No significant differences were found between the Con and Anta-miR-9-5p groups. Since dendritic spines are an important morphological basis for synaptic plasticity, we also examined the dendritic spines in the dentate gyrus using Golgi staining. As expected, we found that CCH significantly decreased

not only the density of dendritic spines but also the percentage of mushroom-type spines (Figure 6A-6C). The pre-administration of anta-miR-9-5p strongly improved the CCH-induced spineogenesis inhibition. These results strongly implied that the *in vivo* suppression of miR-9-5p is able to reverse the synaptic impairments in CCH rats.

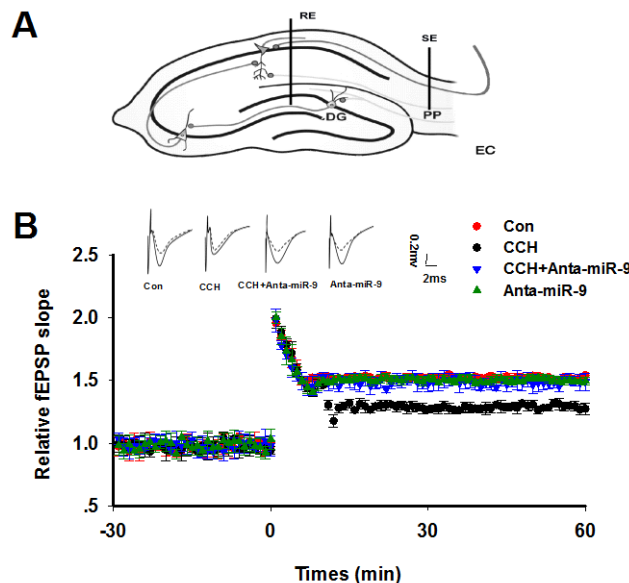


Figure 5: Inhibition of miR-9-5p rescued the LTP inhibition in CCH rats. (A) The diagram for LTP recording. RE: recording electrode; SE: stimulating electrode; PP: perforant path; DG: dentate gyrus. (B) Upper panel: The representative analog traces of evoked potentials before (dashline) and after (solid line) HFS with different treatments are shown. Lower panel: The alterations of LTP represented by normalized slope of EPSP were recorded. The electrophysiology recording was started 30 min (-30), and the HFS was added at 0 min. The data represent means \pm standard error of the mean. CCH, chronic cerebral hypoperfusion; EPSP, excitatory postsynaptic potential; HFS, high frequency stimulation; LTP, long-term potentiation.

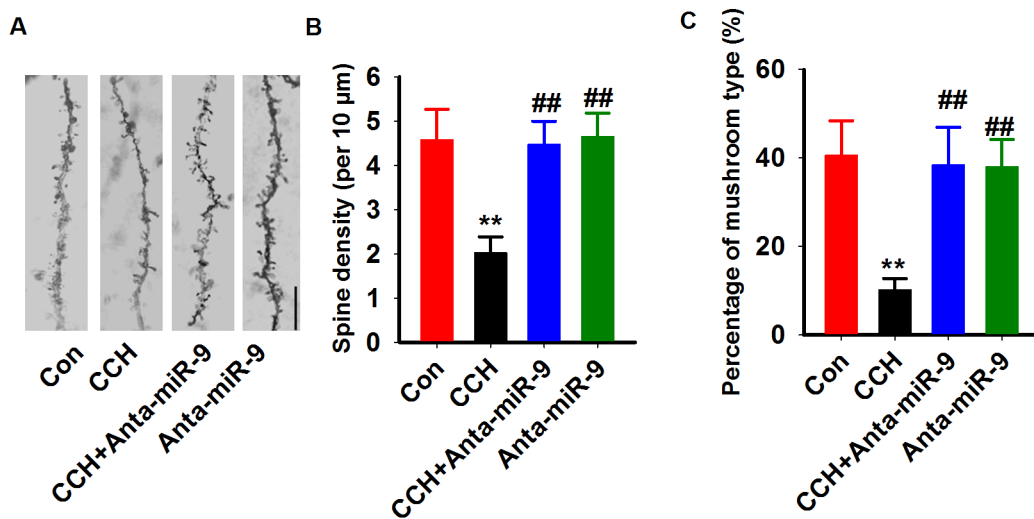


Figure 6: Inhibition of miR-9-5p rescued the dendritic spine abnormalities in CCH rats. (A) Representative images of dendritic spine were captured from Golgi staining of DG region. Bar=20 μ m. (B, C) The quantitative analysis of the density of spines (B) and the percentage of mushroom types (C) were carried. CCH, chronic cerebral hypoperfusion; ** $P < 0.01$ vs. Congroup; ## $P < 0.01$ vs. CCH group.

Reduction of miR-9-5p *in vivo* reduces the cholinergic system in CCH rats

Previous studies suggested that the central cholinergic system dysfunction is involved in memory impairments in CCH rats [20]. Therefore, we measured the effect of suppression of miR-9-5p on ACh levels and activity of AChE and ChAT in the hippocampus of CCH rats. Consistent with previous reports [21], CCH resulted in a significant decrease of ACh levels, increased AChE activity, and a dramatic reduction of ChAT activity in the hippocampus, which confirmed the impaired cholinergic function in CCH. Moreover, we found that suppression of miR-9-5p by anti-miR-9-5p in CCH rats elevated ACh levels and ChAT activity, but decreased AChE activity. No significant differences were found between the Con and anti-miR-9-5p groups (Figure 7A-7C). These data support the behavioral results and suggest that reduction of miR-9-5p may exert its neuroprotective effects by restoring the cholinergic function.

Reduction of miR-9-5p *in vivo* reduces the neuronal loss in CCH rats

It was reported that neuronal loss resulting from apoptotic or necrotic neuronal cell death is a common feature of VaD [22]. We also examined whether the reduction of miR-9-5p *in vivo* could reverse the neuronal loss in CCH rats by using the Nissl staining. Quantitative analysis suggested that CCH induces a dramatic neuronal loss in the hippocampus while pre-administration of anti-miR-9-5p strongly restored the number of neurons in CCH rats (Figure 8A, 8B).

Reduction of miR-9-5p inhibits the oxidative stress level in CCH rats

As the oxidative stress was reported to induce neuronal loss in CCH rats [23], we examined the activities of SOD, GSH-px, and the levels of MDA and T-ROS in the hippocampal homogenates of CCH rats. As predicted, the

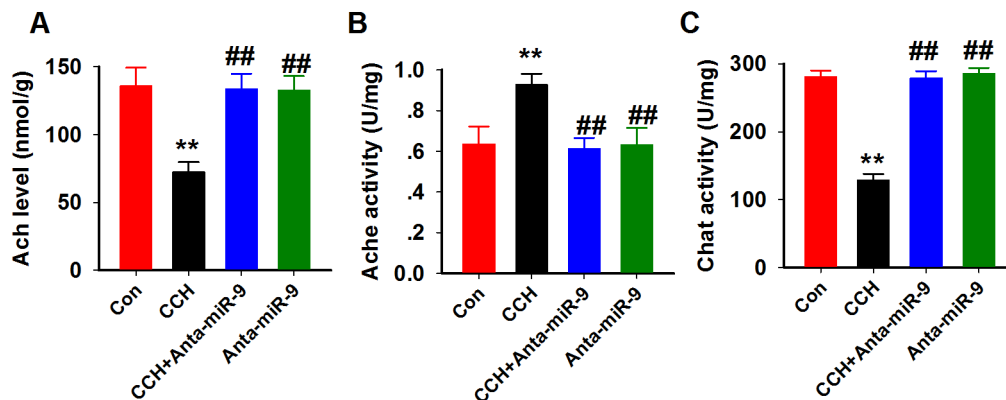


Figure 7: Inhibition of miR-9-5p rescued the cholinergic dysfunction in CCH rats. The cholinergic system function was assayed using ACh (A), AChE (B) and ChAT (C) kits as described above. CCH, chronic cerebral hypoperfusion; ** $P < 0.01$ vs. Congroup; ## $P < 0.01$ vs. CCH group.

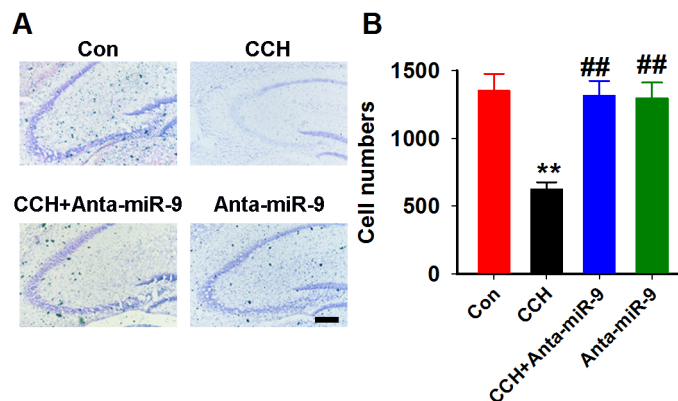


Figure 8: Inhibition of miR-9-5p restored the neuronal loss in CCH rats. (A) A representative image of the hippocampus; scale bar=100 μ m. (B) The quantitative analysis for the whole hippocampus. CCH, chronic cerebral hypoperfusion; ** $P < 0.01$ vs. Congroup; ## $P < 0.01$ vs. CCH group. N=16 slices from 4 rats.

SOD and GSH-px activities were reduced, but the levels of MDA and T-ROS were increased compared with controls. Administration of anti-miR-9-5p significantly restored the activities of SOD and GSH-px and decreased the levels of MDA and T-ROS in the CCH rats (Figure 9A-9D). These data suggested that suppression of miR-9-5p inhibits the oxidative stress level in CCH rats.

DISCUSSION

VaD is thought to be a neurodegenerative disorder caused by multiple vasculotoxic and neurotoxic effects due to diminished cerebral blood flow, which leads to hypoxia and altered permeability of the blood-brain barrier. Several pathological events have been suggested to be the prime risk factors for VaD, such as stroke, cerebral hemorrhage, trauma, chronic diseases like atherosclerosis, large and small vessel disease, and cardioembolic disease [24]. To date, the genetic basis of VaD is not well defined. MiRNAs belong to a class of endogenous, stable, non-coding RNA molecules involved in the regulation of target gene expression at the post-transcriptional level by either the degradation of the RNA or translational arrest [25]. Several miRNAs are expressed specifically in the CNS, where some are proposed to function in neuronal activities such as neurite outgrowth and synapse formation

[26], and in neurodegenerative diseases [27, 28], including VaD [15].

Our results demonstrated that miR-9-5p is critically involved in VaD and that blocking miR-9-5p is sufficient to rescue the learning and memory impairments observed in a VaD rat model. The miR-9-5p gene is evolutionary well conserved. To date, several functional studies on miR-9 have emphasized its role in neuronal development and neurogenesis [29]. For example, miR-9 knock-out mice, in which both miR-9-5p and miR-9-3p are reduced, displayed obvious defects in neurogenesis and abnormal telencephalic structures [30]. It should be mentioned that miR-9-5p and miR-9-3p are abundantly expressed not only in neural progenitors but also in postmitotic neurons [17, 31]; hence the importance of studying the potential role of miR-9 in adulthood and neurological diseases. Indeed, in the postmortem brains of patients with Huntington's disease, the level of miR-9 was decreased [32]. In brains from patients with AD, the level of miR-9 was increased in the temporal lobes, neocortex, and hippocampal regions when compared with age-matched healthy adults [18, 19]. In the current study, we demonstrated an abnormal upregulation of miR-9-5p in both the serum and CSF of patients with VaD, suggesting the potential role of miR-9-5p in VaD progression.

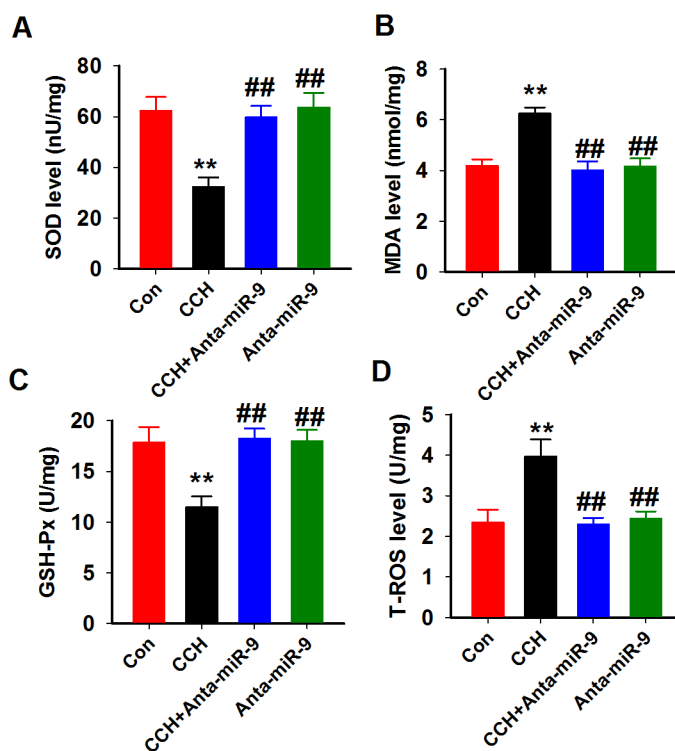


Figure 9: Inhibition of miR-9-5p attenuated the oxidative stress in CCH rats. Four oxidative stress parameters were assayed in the hippocampus homogenates from different groups by using SOD (A), MDA (B), GSH-Px (C) and T-ROS (D) kits described above. CCH, chronic cerebral hypoperfusion; GSH-Px, glutathione peroxidase; MDA, malonic dialdehyde; SOD, superoxide dismutase; T-ROS, reactive oxygen species ** $P < 0.01$ vs. control group; ## $P < 0.01$ vs. CCH group.

Synaptic plasticity and dendritic spines are the basis for learning and memory. Dendritic spines serve as a storage site for synaptic strength and help transmit electrical signals to the neuron's cell body [33]. Spines constitute a specialized compartment that contains multiple signaling complexes, which play important roles in synaptic transmission [34]. The disruption of synapses plays an important role in VaD [35]. Thus, the preservation of dendritic spines predictably restores synaptic plasticity, as well as learning and memory. Recently, in primary culture neurons, Giusti et al. [48] showed that the inhibition of miR-9-5p using the sponge technique impairs dendritic growth and excitatory synaptic transmission. Interestingly, the miR-9-3p sponge had no effect on dendritic growth of cultured neurons [36]. In an independent study, asynergistic effect of miR-9 and miR-124 has been reported in the regulation of dendritic branching via the AKT/GSK3 β pathway by targeting the Rap GTP-binding protein Rap2a [37]. In our study, we found that the administration of miR-9-5p antagomir restores the dendritic spines loss and the synaptic plasticity inhibition in the CCH rats. Moreover, miR-9-5p antagomir did not alter the dendritic spines and LTP in normal rats. These data suggested a discrepancy in the *in vivo* and *in vitro* roles of miR-9-5p in dendritic spines and synaptic plasticity. We propose that such differences may be the result of the more complicated environment in the brain compared with that of cultured neurons.

MATERIALS AND METHODS

Patients and selection criteria

A total of 25 patients with VaD (14 men and 11 women) whose diagnoses were confirmed using the National Institute of Neurological Disorders and Stroke-Association Internationale pour la Recherche et l'Enseignement en Neurosciences (NINDS-AIREN) criteria for VaD [38]. The Mini-Mental State Examination scores of all patients were less than 25. A total of 22 healthy age-matched participants (12 men and 10 women) were recruited from the outpatient setting and served as the control group. The control group was selected from the Medical Examination Centre of the First Affiliated Hospital of Zhengzhou University. In this study, none of the participants presented with hypertension, cardiopathy, diabetes, or renal dysfunction. All experiments using human samples were performed in accordance with the Declaration of Helsinki and the approval of the Institutional Review Board of Zhengzhou University.

Animals and surgery

Male Wistar rats (200–250 g) were obtained from the Animal Center of Zhengzhou University and were kept in standard plastic cages. During one week of

acclimatization, rats were randomly distributed in pairs per cage. They were maintained on *ad libitum* food and water with 12/12 h light/dark cycle. All animal experiments were performed in accordance with the National Institutes of Health Guide for the Care and Use of Laboratory Animals and approved by the Animal Ethics Committee of the Medical School of Zhengzhou University.

After one week of acclimatization, rats were randomly divided into four groups, (1) control rats with the sham operation and vehicle injection (Con), (2) 2VO surgery and vehicle injection (CCH), (3) 2VO surgery with *antamiR-9-5p* injection (CCH+Anta-miR-9-5p), and (4) antamiR-9-5p injection alone (Anta-miR-9-5p). For the 2VO surgery, rats were anesthetized with chloral hydrate (300 mg/kg, intraperitoneal [i.p.]), and bilateral common carotid arteries were gently separated from the carotid sheath and vagal nerves. Each artery was ligated with a 6-0 silk suture. Sham-operated controls received the same operation without ligation. After the procedure, rats were placed on a heating pad until recovery from anesthesia to maintain the body temperature at 37.5 ± 0.5 °C [23]. The antagomir of miR-9-5p (200 nM in aCSF) was administered through stereotaxic brain injection to the DG area (AP -2.0 mm, ML 1.5 mm, DV 2.0 mm) once at 3 months after the surgery. Sham-operated and controlled 2VO animals received the same volume of scrambled control or vehicle. The mortality was 1/17 (5.9%) in the Con group, 3/19 (15.8%) in the CCH group, 2/15 (13.3%) in the CCH+Anta-miR-9 group, and 1/14 (7.1%) in the Anta-miR-9 group. Mortality rates did not differ significantly among the four groups.

RNA isolation and miRNA detection

Total RNA was extracted from the cells and hippocampi using the Trizol Reagent (Invitrogen) according to the manufacturer's instructions. Real-time PCR reactions were performed using an ABI 7500 real-time PCR system (Applied Biosystems, CA, USA). Reverse transcription of the extracted miRNA was performed with miRNA-specific primers using the miRcute miRNA first-strand cDNA synthesis kit, and real-time PCR of miRNAs was performed using the miRcute miRNA qPCR detection kit according to the manufacturer's protocol (TIANGEN BIOTECH, China). U6 was used as endogenous controls and non-neoplastic brain tissues were used for calibration. The primers for detection of human (miRQ0000441-1-1) and rat (miRQ0000142-1-1) miR-9-5p were provided by RiboBio Co., Ltd. (Guangzhou, China) and the primer for U6 are followed: sense: 5'-CTCGCTTCGGCAGCACA; anti-sense: 5'-AACGCTTCACGAATTTGCGT).

Morris water maze

The Morris water maze (MWM) task was carried out at 3 months post-surgery [39, 40]. The maze consisted of a circular water tank (120 cm in diameter and 60

cm in depth) that was filled to a depth of 32 cm with opaque water and maintained at 22–26 °C. A hidden circular platform (10 cm in diameter) was submerged approximately 1.5 cm below the surface of the water and was kept at the same location in the southwest quadrant throughout the training period. All rats (including the sham-operated group) were subjected to daily MWM tests after completing a visual acuity test, as described previously [41]. Spatial training of the hidden platform in the water maze was performed for 6 consecutive days. Each rat received two trials per day with an intertrial interval of 1 min. The starting position (east, west, south, or north) for each trial was pseudo-randomly chosen and counterbalanced across all experimental groups. The swimming paths of the rats were monitored by a video camera linked to a computer. For each training trial, the latency to escape onto the hidden platform was recorded. The rats were given a maximum of 60 s to find the hidden platform. If the rat failed to find the platform within 60 s, the training was terminated and a maximum score of 60 s was assigned. Each rat was placed on the platform for 30 s before being removed from the water maze. For the probe trial on the 9th day of training [42], rats were subjected to a single 60-s swim without a hidden platform during the whole task, and the following durations were recorded: (1) time spent in the target quadrant where the platform had been placed during training, (2) the crossing times to the platform region, and (3) the initial time to cross the platform region. Swimming speed was also analyzed to evaluate motor ability [43].

Step-down inhibitory avoidance task

Animals were subjected to training and test sessions in a step-down inhibitory avoidance task with an interval of 24 h. This task involves learning not to stepdown from a platform in order to avoid a mild foot shock. The inhibitory avoidance apparatus was an acrylic box (30 cm × 30 cm × 30 cm) with a floor consisting of parallel stainless steel bars (5 mm diameter) spaced 1 cm apart. A platform (5-cm wide × 5-cm high) was placed at one corner on the floor. Rats were placed on the platform and the time latency to step-down on the grid with all four paws was measured with an automatic device. During the training sessions, immediately after stepping down on the grid, the animals received an electrical foot shock (0.4 mA, 1.0 s scrambled). During the test sessions, no foot shock was delivered and step-down latency (with a ceiling of 180 s) was used as a measure of memory retention, as described in previous reports. The test sessions were performed 24 h after training to evaluate long-term memory [44, 45].

Long-term potentiation recording

The long-term potentiation (LTP) recording and assay methods were performed as previously described

[46]. Briefly, animals were anesthetized with chloral hydrate (300 mg/kg, i.p.) and placed on a stereotaxic instrument. The stimulating electrode was placed in the perforant path (anterior-posterior [AP] -7.0mm, mediolateral [ML] 4.5mm, dorsoventral [DV] 3.5 mm) and the recording electrode in the dentate gyrus region (AP -2.0 mm, ML 1.5 mm, DV 2.0 mm) of the hippocampus. The initial baseline responses were obtained by delivering a single pulse of stimulation once every 10 s. For each recording experiment, a stable baseline for at least 30 min was required before the application of conditioning stimuli. LTP was elicited using high-frequency stimulation (HFS) consisting of four trains of 50 pulses delivered at 200 Hz with a 2 s intertrain interval. The slope of the excitatory postsynaptic potential (EPSP) was recorded for 60 min and calculations were done by a computerized program (RM6240BD; Chengdu, China).

Golgi staining

Golgi staining was performed as previously described [47]. Briefly, tissue slices (~4-mm thick) were placed in a solution containing 5% chloral hydrate, 5% potassium dichromate, 10% formalin in ddH₂O for 3 days and then subjected to 1% silver nitrate under continuous vacuum for 4 days. Subsequently, brain tissues were cut into 40-μm thick sections with a vibratome and analyzed using a light microscope (Olympus BX60, Tokyo, Japan) with a 100X objective lens. The number of dendritic spines and the percent of mushroom-like spines on hippocampal DG pyramidal neurons were analyzed blindly (i.e. without knowledge of the treatment groups). For each experimental group, a minimum of 40 cells per animal (n = 4) were analyzed by Image-Pro Plus 6.0 software. The criteria for the spine analysis were defined according to a previous study [48].

ELISA

Twenty-four hours after the behavioral testing, rats were sacrificed under deep anesthesia. The hippocampi were subsequently dissected on ice and stored at -80 °C for further biochemical assays. The hippocampal samples were prepared as previously described [49]. For the analysis of the cholinergic function, the activity of choline acetyltransferase (ChAT) and acetylcholinesterase (AChE) was measured spectrophotometrically using commercial assay kits according to the manufacturer's instructions (Cat. No. A079-1, A024, Nanjing Jiancheng Biotech. Inc., Nanjing, China). The level of ACh in the hippocampal supernatant was detected with an ELISA kit according to the manufacturer's instructions (Cat. No. A105-1, Nanjing Jiancheng Biotech. Inc., Nanjing, China). To measure oxidative stress, the activities of superoxide dismutase (SOD; Cat. No. A001-3), glutathione peroxidase (GSH-Px; Cat. No. A005), reactive oxygen

species (T-ROS; Cat. No. E004), and the levels of malonic dialdehyde (MDA; Cat. No. A003-1) were examined using commercial kits (Nanjing Jiancheng Biotech., Inc., Nanjing, China).

Nissl staining

The rats were anesthetized with an i.p. overdose of chloral hydrate and then perfused transcardially with 0.9% Sodium Chloride at 4 °C followed by 4% paraformaldehyde in 0.1 M phosphate-buffer (PB, pH 7.4). The whole brains were removed and postfixed in 4% paraformaldehyde at 4 °C for another 24 h. After dehydration in 30% and 40% sucrose until sunk, the brains were rapidly frozen in isopentane and 25- μ m thick coronal sections were cut on a cryostat (CM 1950, Leica, Heidelberg, Germany). All the sections were used for Nissl staining, which was performed with 0.1% cresyl violet (Sigma, St Louis, MO, USA) to evaluate neuronal damage in the hippocampus. For cell counting, the NIH Image J software was used as previously reported [50].

Statistical analysis

All data were expressed as the mean \pm standard deviation (SD). Data were analyzed using two-way analysis of variance (ANOVA) followed by Duncan's multiple range test when appropriate. *P* values less than 0.05 ($P < 0.05$) were considered statistically significant.

Author contributions

N.W., K.Z., J.J.X. and K.S.C initiated and organized the study. N.W., K.Z., R.X., S.M., H.Y. R., H.F.H., W.W.W., performed the main experimental work. N.W. analysed the data and performed statistical analysis. N.W., K.Z., J.J.X. and K.S.C wrote the manuscript. All authors approved the final version of the manuscript.

CONFLICTS OF INTEREST

The authors declare that they have no competing interests.

FUNDING

This work was supported by the National Natural Science Foundation of China (81600944, U1304804, 81570199), the Youth Innovation Fund of The First Affiliated Hospital of Zhengzhou University and the key research projects of HeNan higher education (17A310010, 17A310029).

REFERENCES

1. Burns A, Iliffe S. Dementia. *BMJ*. 2009; 338:b75.

2. Battistin L, Cagnin A. Vascular cognitive disorder. A biological and clinical overview. *Neurochem Res*. 2010; 35:1933-1938.

3. Roher AE, Debbins JP, Malek-Ahmadi M, Chen K, Pipe JG, Maze S, Belden C, Maarouf CL, Thiyyagura P, Mo H, Hunter JM, Kokjohn TA, Walker DG, et al. Cerebral blood flow in Alzheimer's disease. *Vasc Health Risk Manag*. 2012; 8:599-611.

4. Hoyer S. Senile dementia and Alzheimer's disease. Brain blood flow and metabolism. *Prog Neuropsychopharmacol Biol Psychiatry*. 1986; 10:447-478.

5. de la Torre JC. Cerebrovascular and cardiovascular pathology in Alzheimer's disease. *Int Rev Neurobiol*. 2009; 84:35-48.

6. Gorelick PB, Scuteri A, Black SE, Decarli C, Greenberg SM, Iadecola C, Launer LJ, Laurent S, Lopez OL, Nyenhuis D, Petersen RC, Schneider JA, Tzourio C, et al. Vascular contributions to cognitive impairment and dementia: a statement for healthcare professionals from the american heart association/american stroke association. *Stroke*. 2011; 42:2672-2713.

7. de la Torre JC. Alzheimer disease as a vascular disorder: nosological evidence. *Stroke*. 2002; 33:1152-1162.

8. Pantoni L, Garcia JH. Pathogenesis of leukoariosis: a review. *Stroke*. 1997; 28:652-659.

9. Kalara RN. Cerebral vessels in ageing and Alzheimer's disease. *Pharmacol Ther*. 1996; 72:193-214.

10. Ogata J. Vascular dementia: the role of changes in the vessels. *Alzheimer Dis Assoc Disord*. 1999; 13:S55-58.

11. Kitagawa K, Yagita Y, Sasaki T, Sugiura S, Omura-Matsuoka E, Mabuchi T, Matsushita K, Hori M. Chronic mild reduction of cerebral perfusion pressure induces ischemic tolerance in focal cerebral ischemia. *Stroke*. 2005; 36:2270-2274.

12. Bartel DP. MicroRNAs: genomics, biogenesis, mechanism, and function. *Cell*. 2004; 116:281-297.

13. He L, Hannon GJ. MicroRNAs: small RNAs with a big role in gene regulation. *Nat Rev Genet*. 2004; 5:522-531.

14. Bushati N, Cohen SM. microRNA functions. *Annu Rev Cell Dev Biol*. 2007; 23:175-205.

15. Ragusa M, Bosco P, Tamburello L, Barbagallo C, Condorelli AG, Tornitore M, Spada RS, Barbagallo D, Scalia M, Elia M, Di Pietro C, Purrello M. miRNAs plasma profiles in vascular dementia: biomolecular data and biomedical implications. *Front Cell Neurosci*. 2016; 10:51.

16. Femminella GD, Ferrara N, Rengo G. The emerging role of microRNAs in Alzheimer's disease. *Front Physiol*. 2015; 6:40.

17. Yuva-Aydemir Y, Simkin A, Gascon E, Gao FB. MicroRNA-9: functional evolution of a conserved small regulatory RNA. *RNA Biol*. 2011; 8:557-564.

18. Lukiw WJ. Micro-RNA speciation in fetal, adult and Alzheimer's disease hippocampus. *Neuroreport*. 2007; 18:297-300.

19. Sethi P, Lukiw WJ. Micro-RNA abundance and stability in human brain: specific alterations in Alzheimer's disease temporal lobe neocortex. *Neurosci Lett.* 2009; 459:100-104.
20. Deiana S, Platt B, Riedel G. The cholinergic system and spatial learning. *Behav Brain Res.* 2011; 221:389-411.
21. Ni JW, Matsumoto K, Li HB, Murakami Y, Watanabe H. Neuronal damage and decrease of central acetylcholine level following permanent occlusion of bilateral common carotid arteries in rat. *Brain Res.* 1995; 673:290-296.
22. Xu L, Di Q, Zhang Y. Cell cycle proteins preceded neuronal death after chronic cerebral hypoperfusion in rats. *Neurol Res.* 2008; 30:932-939.
23. Saxena AK, Abdul-Majeed SS, Gurtu S, Mohamed WM. Investigation of redox status in chronic cerebral hypoperfusion-induced neurodegeneration in rats. *Appl Transl Genom.* 2015; 5:30-32.
24. Iadecola C. The pathobiology of vascular dementia. *Neuron.* 2013; 80:844-866.
25. De Smaele E, Ferretti E, Gulino A. MicroRNAs as biomarkers for CNS cancer and other disorders. *Brain Res.* 2010; 1338:100-111.
26. Delay C, Mandemakers W, Hebert SS. MicroRNAs in Alzheimer's disease. *Neurobiol Dis.* 2012; 46:285-290.
27. Eacker SM, Dawson TM, Dawson VL. Understanding microRNAs in neurodegeneration. *Nat Rev Neurosci.* 2009; 10:837-841.
28. Sonntag KC. MicroRNAs and deregulated gene expression networks in neurodegeneration. *Brain Res.* 2010; 1338:48-57.
29. Coolen M, Katz S, Bally-Cuif L. miR-9: a versatile regulator of neurogenesis. *Front Cell Neurosci.* 2013; 7:220.
30. Wheeler BM, Heimberg AM, Moy VN, Sperling EA, Holstein TW, Heber S, Peterson KJ. The deep evolution of metazoan microRNAs. *Evol Dev.* 2009; 11:50-68.
31. Liu DZ, Ander BP, Tian Y, Stamova B, Jickling GC, Davis RR, Sharp FR. Integrated analysis of mRNA and microRNA expression in mature neurons, neural progenitor cells and neuroblastoma cells. *Gene.* 2012; 495:120-127.
32. Packer AN, Xing Y, Harper SQ, Jones L, Davidson BL. The bifunctional microRNA miR-9/miR-9* regulates REST and CoREST and is downregulated in Huntington's disease. *J Neurosci.* 2008; 28:14341-14346.
33. Bourne JN, Harris KM. Balancing structure and function at hippocampal dendritic spines. *Ann Rev Neurosci.* 2008; 31:47-67.
34. Kennedy MJ, Ehlers MD. Organelles and trafficking machinery for postsynaptic plasticity. *Ann Rev Neurosci.* 2006; 29:325-362.
35. Li H, Wang J, Wang P, Rao Y, Chen L. Resveratrol reverses the synaptic plasticity deficits in a chronic cerebral hypoperfusion rat model. *J Stroke Cerebrovasc Dis.* 2016; 25:122-128.
36. Giusti SA, Vogl AM, Brockmann MM, Vercelli CA, Rein ML, Trumbach D, Wurst W, Cazalla D, Stein V, Deussing JM, Refojo D. MicroRNA-9 controls dendritic development by targeting REST. *Elife.* 2014.
37. Xue Q, Yu C, Wang Y, Liu L, Zhang K, Fang C, Liu F, Bian G, Song B, Yang A, Ju G, Wang J. miR-9 and miR-124 synergistically affect regulation of dendritic branching via the AKT/GSK3beta pathway by targeting Rap2a. *Sci Rep.* 2016; 6:26781.
38. Roman GC, Tatemichi TK, Erkinjuntti T, Cummings JL, Masdeu JC, Garcia JH, Amaducci L, Orgogozo JM, Brun A, Hofman A, Moody DM, O'Brien MD, Yamaguchi T, et al. Vascular dementia: diagnostic criteria for research studies. Report of the NINDS-AIREN International Workshop. *Neurology.* 1993; 43:250-260.
39. Hai J, Su SH, Lin Q, Zhang L, Wan JF, Li H, Chen YY, Lu Y. Cognitive impairment and changes of neuronal plasticity in rats of chronic cerebral hypoperfusion associated with cerebral arteriovenous malformations. *Acta Neurol Belg.* 2010; 110:180-185.
40. Melani A, Cipriani S, Corti F, Pedata F. Effect of intravenous administration of dipyrindamole in a rat model of chronic cerebral ischemia. *Ann N Y Acad Sci.* 2010; 1207:89-96.
41. Walsh CM, Booth V, Poe GR. Spatial and reversal learning in the Morris water maze are largely resistant to six hours of REM sleep deprivation following training. *Learn Mem.* 2011; 18:422-434.
42. Hu J, Huang HZ, Wang X, Xie AJ, Wang X, Liu D, Wang JZ, Zhu LQ. Activation of glycogen synthase kinase-3 mediates the olfactory deficit-induced hippocampal impairments. *Mol Neurobiol.* 2015; 52:1601-1617.
43. Peng Y, Xu S, Chen G, Wang L, Feng Y, Wang X. 1-3-n-Butylphthalide improves cognitive impairment induced by chronic cerebral hypoperfusion in rats. *J Pharmacol Exp Ther.* 2007; 321:902-910.
44. Lucena GM, Prediger RD, Silva MV, Santos SN, Silva JF, Santos AR, Azevedo MS, Ferreira VM. Ethanolic extract from bulbs of *Cipura paludosa* reduced long-lasting learning and memory deficits induced by prenatal methylmercury exposure in rats. *Dev Cogn Neurosci.* 2013; 3:1-10.
45. Zhou P, Chen Z, Zhao N, Liu D, Guo ZY, Tan L, Hu J, Wang Q, Wang JZ, Zhu LQ. Acetyl-L-carnitine attenuates homocysteine-induced Alzheimer-like histopathological and behavioral abnormalities. *Rejuvenation Res.* 2011; 14:669-679.
46. Wang SH, Liao XM, Liu D, Hu J, Yin YY, Wang JZ, Zhu LQ. NGF promotes long-term memory formation by activating poly (ADP-ribose) polymerase-1. *Neuropharmacology.* 2012; 63:1085-1092.
47. Wang X, Wang ZH, Wu YY, Tang H, Tan L, Wang X, Gao XY, Xiong YS, Liu D, Wang JZ, Zhu LQ. Melatonin attenuates scopolamine-induced memory/synaptic disorder

- by rescuing EPACs/miR-124/Egr1 pathway. *Mol Neurobiol.* 2013; 47:373-381.
48. Liu D, Tang H, Li XY, Deng MF, Wei N, Wang X, Zhou YF, Wang DQ, Fu P, Wang JZ, Hebert SS, Chen JG, Lu Y, Zhu LQ. Targeting the HDAC2/HNF-4A/miR-101b/AMPK pathway rescues tauopathy and dendritic abnormalities in Alzheimer's disease. *Mol Ther.* 2017; 25:752-764.
49. Wei N, Xiao L, Xue R, Zhang D, Zhou J, Ren H, Guo S, Xu J. MicroRNA-9 mediates the cell apoptosis by targeting Bcl2l11 in ischemic stroke. *Mol Neurobiol.* 2016; 53:6809-6817.
50. Miller DJ, Balam P, Young NA, Kaas JH. Three counting methods agree on cell and neuron number in chimpanzee primary visual cortex. *Front Neuroanat.* 2014; 8:36.